TABLE 1. Résumé of AVP immunoreactivity of the mouse hypothalamus and neurohypophysis during fetal and postnatal development

Age (days)	Hypothalamus					Neurohypophysis		
	SON	RCN	PVN	SCN	Acc.	ME		PN
						f.l.	e.l.	
Fetal age								
14	±	+	−	−	−	−	−	−
15	+	+	+	−	±	+	−	+
16	+	+	+	±	+	+	−	+
17	++	++	+	±	++	++	+	++
18	++	++	+	±	++	++	+	++
Postnatal age								
2	++	++	++	+	++	++	++	++
14	+++	+++	+++	++	++	+++	++	+++
30	+++	+++	+++	++	+++	+++	+	+++
90	+++	+++	+++	++	+++	+++	+	+++

Staining intensity was arbitrarily graded as: −, none; +, weak; ++, moderate; +++, intense.
Abbreviations: SON, supraoptic nucleus; RCN, retrochiasmatic nucleus; PVN, paraventricular nucleus; SCN, suprachiasmatic nucleus; Acc., accessory nuclei; ME, median eminunce; f.l., fiber layer; e.l., external layer; PN, pars nervosa.
Accessory nuclei are consisted of the anterior commissural nucleus, nucleus circularis, and anterior and posterior fornical nuclei.

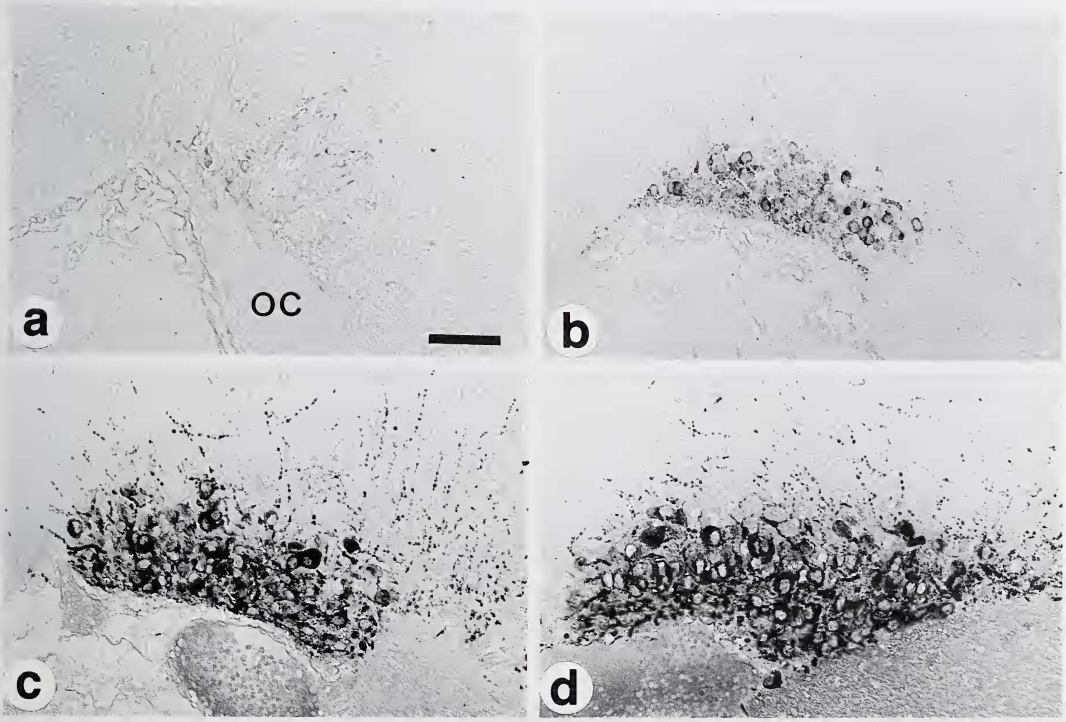

FIG. 2. Frontal sections of the right supraoptic nucleus during development. Stained with anti-AVP serum. a, FA 15; b, FA 18; c, PA 14; d, PA 90. OC, optic chiasma. Bar: 50 μm.

neurons in the RCN was more than in the SON. There was no AVP immunoreactivity in other nuclei of the hypothalamus.

On FA 15, the AVP immunoreactivity of the SON and RCN neurons became apparent, though the stainability was still weak (Figs. 2a and 3a). Each cell nucleus was enclosed in a thin rim of cytoplasm. There were some neurons which did not completely settle in the SON. A few neurons in the PVN and internuclear magnocellular (accessory) nuclei between the SON and PVN became first stainable on this day. But no immunoreactive material was detected in the SCN.

AVP immunoreactivity in the PVN on FA 16 was almost the same as that on FA 15 (Fig. 4a). Weak AVP immunoreactivity was first detected in the SCN in one of five FA 16 fetuses. Adult-type partition of immunoreactive neurons in the RCN into medial and lateral groups was observed as early as this fetal day.

Immunostainability of the SON and RCN neurons increased on FA 17 (Table 1). The SCN neurons were only weakly stainable with the antiserum in three fetuses on FA 17 (Fig. 5a).

On FA 18, many neurons in the SON and RCN accumulated the AVP-immunoreactive material in their cytoplasmic rim. Axonal fibers from the neurons with the bead-like deposits were encountered in these nuclei (Figs. 2b and 3b).

Numbers of immunoreactive neurons (Fig. 8). During the fetal life, magnocellular neurons in the SON, RCN and PVN did not grow as large as those of the adult. The number of immunoreactive neurons generally increased during the gestation period. In the SON and RCN, the number of AVP-immunoreactive neurons rapidly increased between FA 14 and FA 18. More immunostained cells were counted in the SON than in the RCN,

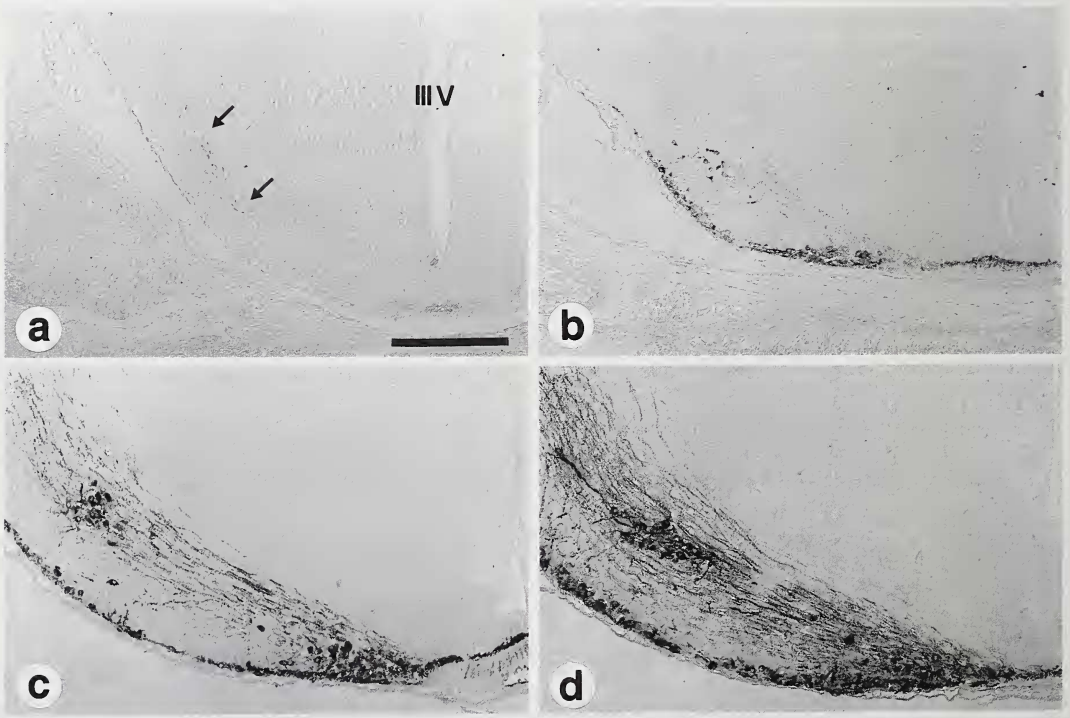

FIG. 3. Frontal sections of the right retrochiasmatic nucleus during development. Stained with anti-AVP serum. a, FA 15; b, FA 18; c, PA 14; d, PA 90. Arrows show the weakly AVP-immunoreactive neurons. IIIV; third ventricle. Bar: 200 μm.

FIG. 4. Frontal sections of the right paraventricular nucleus during development. Stained with anti-AVP serum. a, FA 16; b, PA 2; c, PA 14; d, PA 90. IIIV, third ventricle. Bar: 50 μm. (in page 1025)

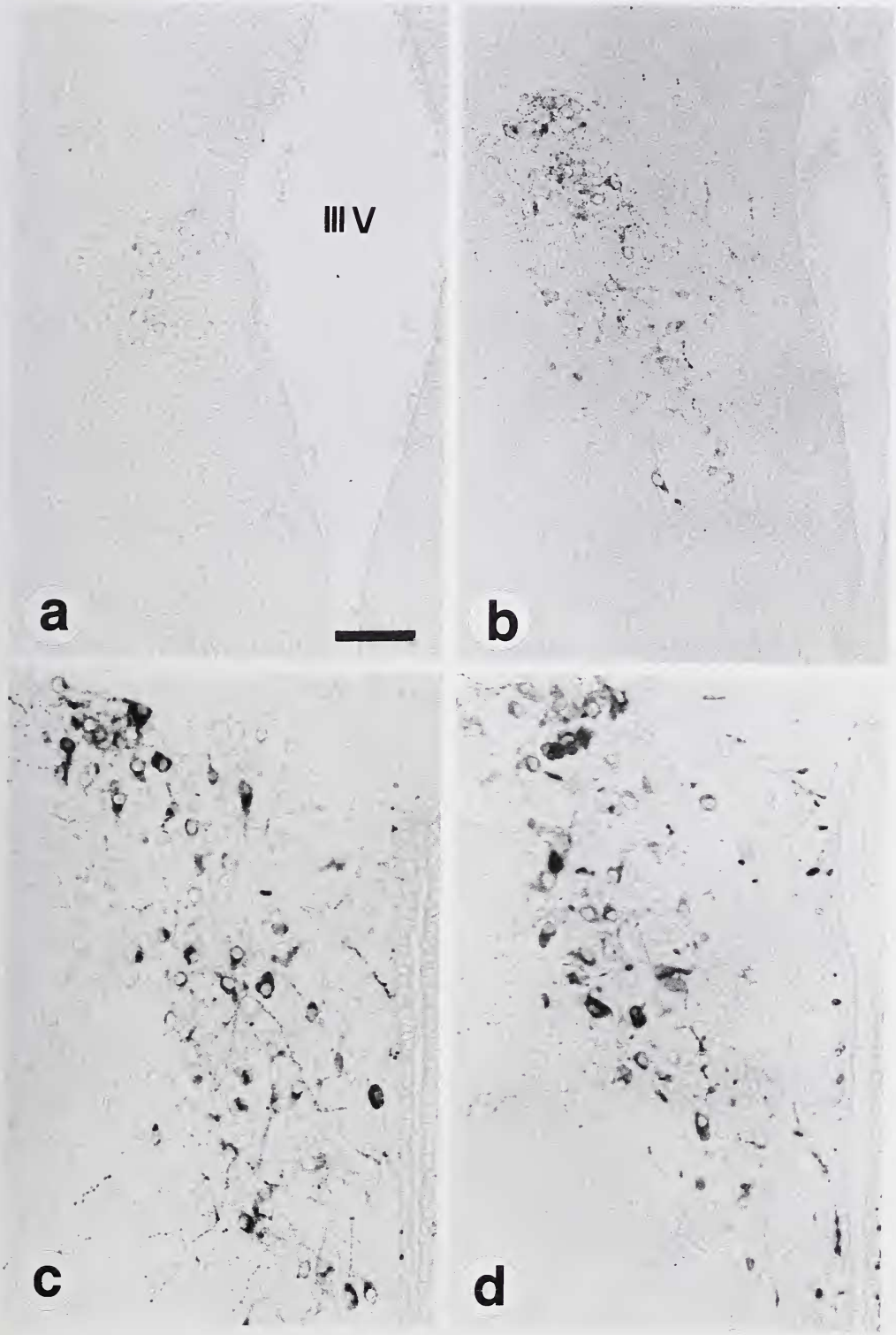
III V
a
b
c
d

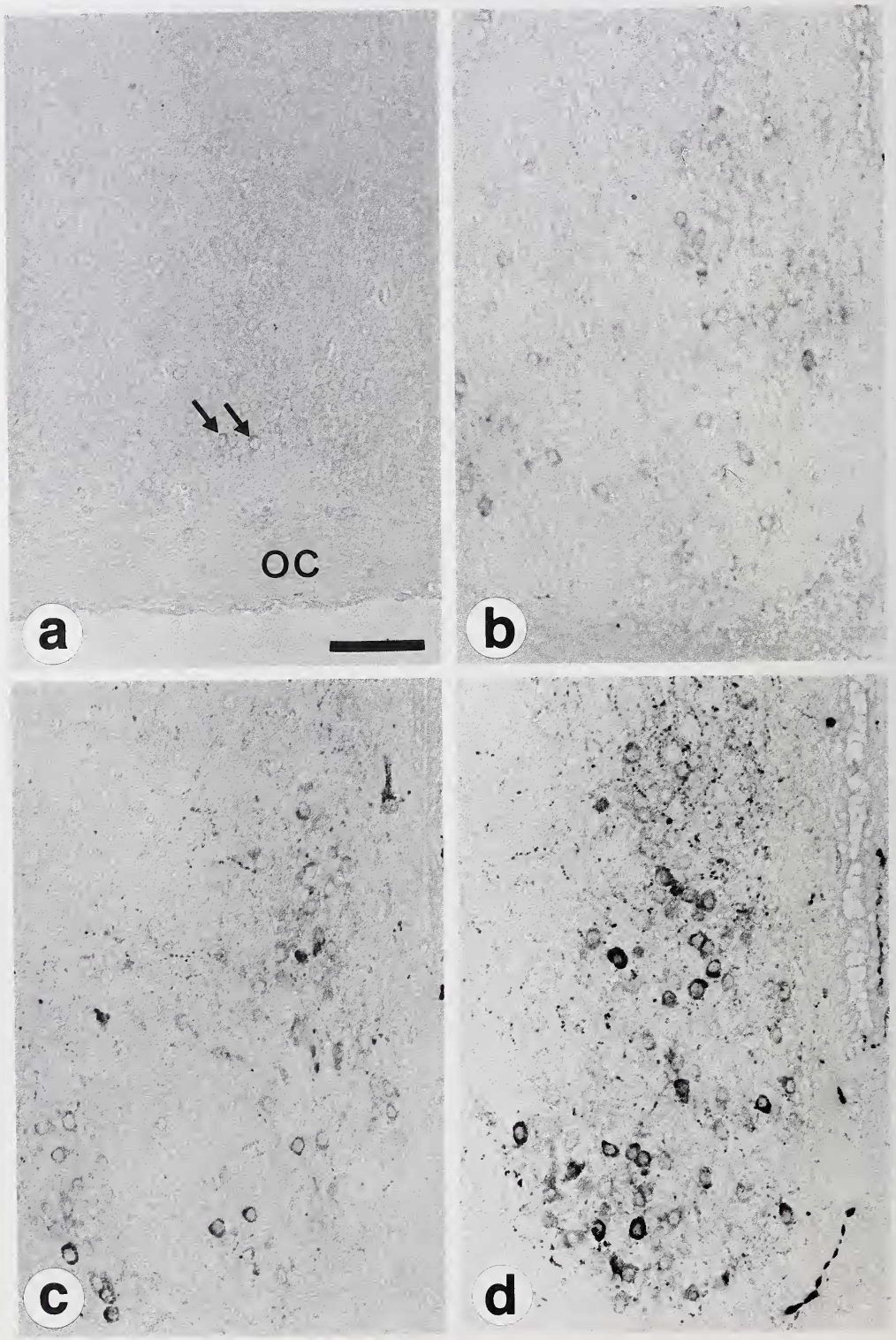
OC
a
b
c
d

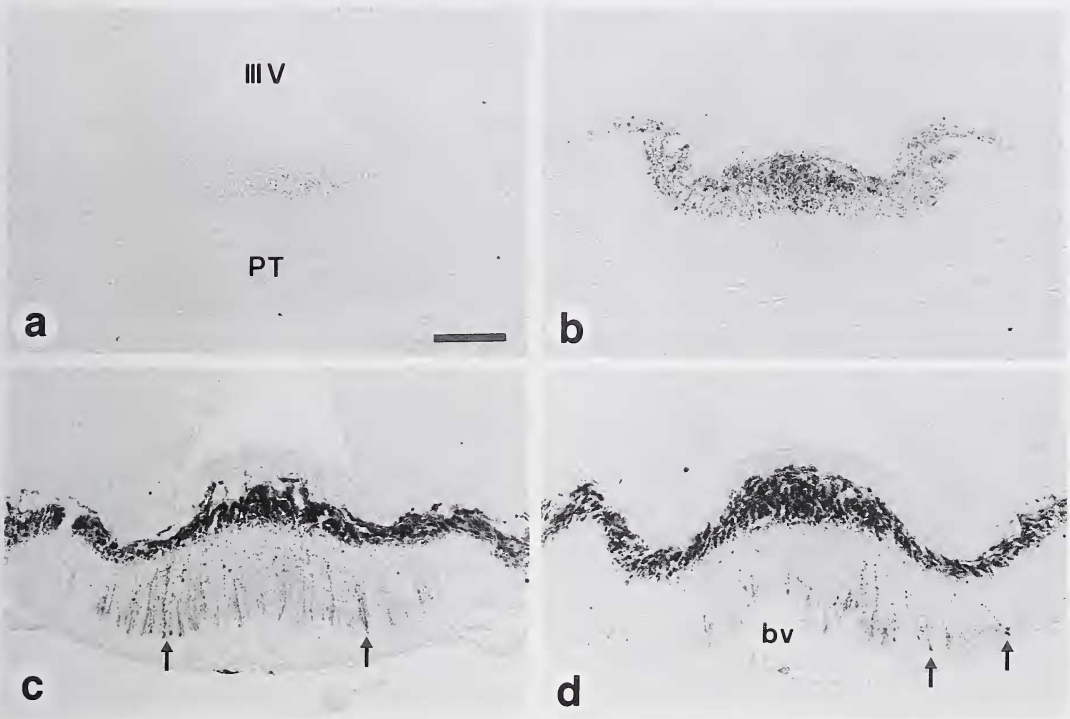

FIG. 6. Frontal sections of the median eminence during development. Stained with anti-AVP serum. a, FA 15; b, FA 18; c, PA 14; d, PA 90. Arrows show the AVP-immunoreactive axonal termini in the external layer of the median eminence. IIIV, third ventricle; PT, pars tuberalis; bv, blood vessel. Bar: 50 μm.

except on FA 14. In comparison with these nuclei, the numbers of immunoreactive neurons in the PVN, SCN and accessory nuclei showed a slight increase during the fatal life.

Development of the neurohypophysis. With the maturation of AVP-producing neurons, stainability of the ME and PN was also enhanced. AVP immunoreactivity was first detected on FA 15 in the ME and the peripheral edge of the PN (Figs. 6a and 7a). AVP-immunoreactive axonal termini in the external layer of the ME first appeared on FA 18 (Fig. 6b). Immunoreactive area in the PN indicated the preferential peripheral localization at the early stage of development (Fig. 7ab), and it gradually expanded to the central area. However, even on FA 17 and 18 strong immunoreactivity was confined to the peripheral area (Fig. 7cd).

Postnatal life

Development of the hypothalamus. After birth, the maturation of magnocellular neurons in the SON, RCN and PVN further advanced. The cells were hypertrophied and became oval in shape. The hypertrophy was generally accompanied by the accumulation of AVP-immunoreactive material (Figs. 2cd, 3cd and 4d).

On PA 2, immunoreactive area of the PVN became triangular in shape like that of the adult. With the rapid increase in the number of immunoreactive cells in the PVN between PA 2 and PA 14, stainability of the cells also increased (Fig. 4bc).

In the parvocellular SCN the increase in AVP immunoreactivity occurred mainly during postna-

FIG. 5. Frontal sections of the right suprachiasmatic nucleus during development. Stained with anti-AVP serum. a, FA 17; b, PA 14; c, PA 30; d, PA 90. Arrows show the weakly AVP-immunoreactive neurons. OC, optic chiasma. Bar: 50 μm. (in page 1026)

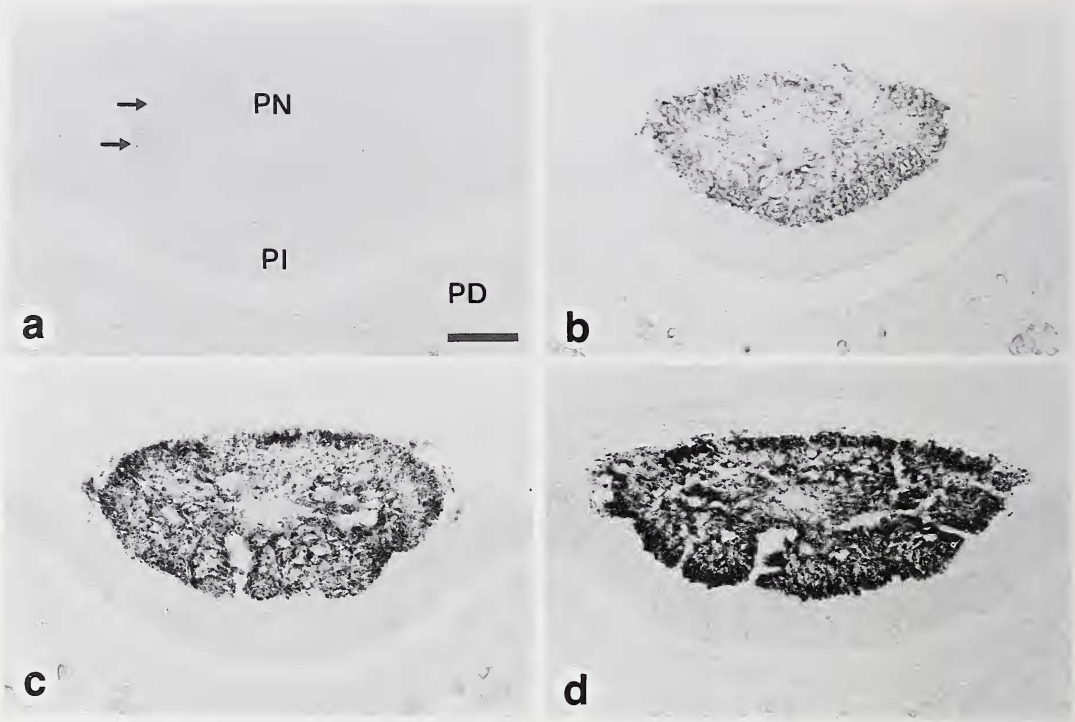

FIG. 7. Frontal sections of the pars nervosa (PN) during fetal development. Stained with anti-AVP serum. a, FA 15; b, FA 16; c, FA 17; d, FA 18. Arrows show the AVP-immunoreactive area in the periphery of the PN. Weak non-specific reactivity is seen in the pars intermedia (PI) and pars distalis (PD). Bar: 50 μm.

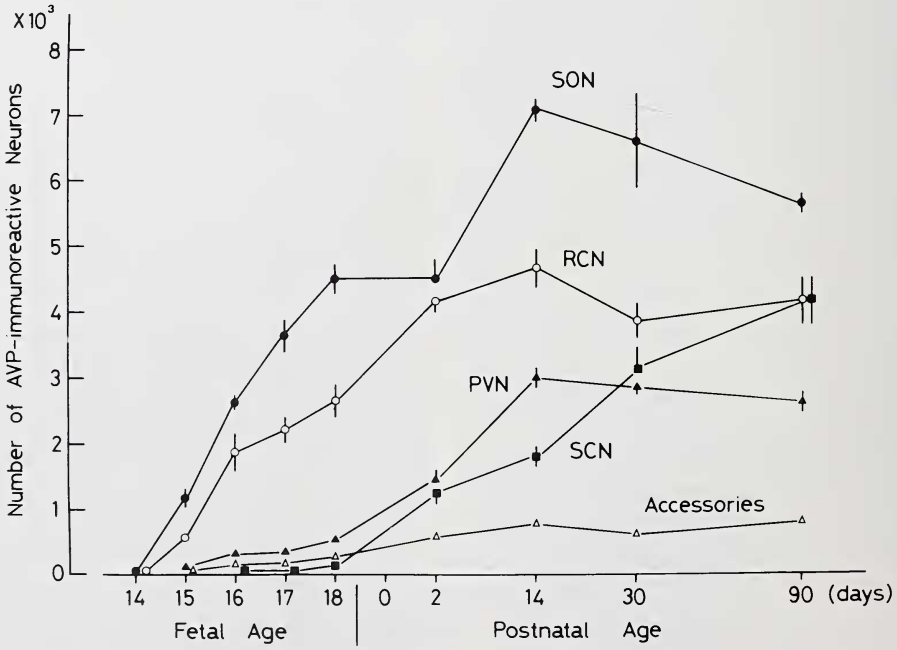

FIG. 8. Total number of AVP-immunoreactive neurons in the mouse hypothalamus during fetal and postnatal development. Vertical bars indicate the standard errors of the means. The number of animals was five in all age groups. For abbreviations, see the footnotes of Table 1.

tal development (Table 1). Adult-like distribution consisted of the dorso-medial and ventro-lateral groups was seen on PA 30 (Fig. 5c). Many neurons were weakly stained with the antiserum (Fig. 5d).

Bead-like structure of immunoreactive axons became more frequently encountered in the vicinity of the neurons as the accumulation in the perikarya proceeded. For example, the axons containing AVP-immunoreactive material were found in the PVN and SCN (Fig. 5b) on PA 2 and PA 14, respectively.

Most of the neurons of the accessory nuclei were strongly immunoreactive to anti-AVP serum after birth (Table 1).

Numbers of immunoreactive neurons (Fig. 8). The numbers of AVP-immunoreactive neurons in the RCN and accessory nuclei were stable after PA 2. The numbers in the SON and PVN continued to increase until PA 14 and maintained the level of PA 14 thereafter. However, there was a marked difference in the number of AVP-immunoreactive neurons between the SON and PVN. On the other hand, the number of immunoreactive neurons of the SCN continued to increase until PA 90.

Development of the neurohypophysis. AVP immunoreactivity in the fiber layer of the ME and the PN on PA 14 was stronger than on PA 2, but after PA 14 it was almost constant (Table 1). Postnatal development of the external layer of the ME was marked (Fig. 6c). Many AVP-immunoreactive axons with the bead-like deposits grew out from the fiber layer down to the external layer of the ME, and their termini were settled on the primary capillary plexus (Fig. 6d). AVP immunoreactivity in the external layer of the ME has decreased concomitantly with the development of the ME (Table 1).

DISCUSSION

Several investigators have reported the developmental changes of neurons in the hypothalamic nuclei by means of [^{3}H]-thymidine autoradiography [28, 29]. In the rat, Ifft [28]* showed that the neurons of the SON became visible between FA 11 and FA 15, those of the RCN between FA 11 and FA 17, those of the PVN between FA 11 and FA 16, and those of the SCN between FA 11 and FA 17 in the matrix layer surrounding the third ventricle. On the other hand, in the mouse of which gestation period is about two days shorter than that of the rat, Okamura *et al.* [29] reported the time of origin of AVP-producing neurons by combined technique of immunocytochemistry and autoradiography. According to their results, AVP-producing neurons in the SON and PVN seem to differentiate between FA 10 and FA 12. In the SCN the neurons proliferate between FA 10 and FA 14, and most of them appear to be produced in the latter half of this period. After the final division in the matrix layer, hypothalamic neurons migrate to occupy the final loci within 24 hr [30]. In addition, Altman and Bayer [31] suggested that there is a general lateral-to-medial internuclear differentiation gradient of the hypothalamic neurons.

In the present study, AVP-immunoreactive neurons were first detected on FA 14 in the SON and RCN but not in other nuclei of the mouse hypothalamus. Evidently, there was a time lag between the stage of neuronal proliferation and the stage of AVP synthesis. Since we could not observe immunoreactivity in the neurons migrating to the SON and RCN, the settlement of cells in the final loci may have some positive effects on the initiation of AVP synthesis. Silverman *et al.* [32], however, reported that on FA 13 some presumptive SON neurons synthesized the AVP carrier protein, neurophysin, while they were still migrating. Because of the limit of sensitivity of immunocytochemical reaction, it is possible that there was an earlier onset of AVP synthesis in the hypothalamic neurons and/or that many more cells contained subdetectable levels of AVP. In fact, a very small amount of AVP was detected by radioimmunoassay in the mouse brain on FA 13 (our unpublished observation). If immunocytochemistry using antibodies to the hormone precursor or autoradiography using the labelled oligonucleotide probe to AVP messenger RNA was performed, the time of cytodifferentiation of AVP neurons might be found at earlier embryonic life.

* Fetal ages in the cited paper were rearranged for convenience of comparison with the present study, so that the day when vaginal plug was observed was designated as FA 0.

Magnocellular neurons developed rapidly during the fetal life. Especially in the SON and RCN, the number of AVP-immunoreactive neurons increased linearly during the fetal life and reached the adult level on PA 2. On the other hand, the PVN appeared to develop later than the SON and RCN, although the number of AVP-immunoreactive neurons of the PVN reached the adult level on PA 14. These results are consistent with the previous studies [21, 22, 32]. Since the neurons of the SON, RCN and PVN cease to divide and start migration almost at the same time [28, 29, 31, 33], it needed to be clarified why the SON and RCN neurons should be so advanced in increasing their numbers. The SCN neurons became immunoreactive in one animal on FA 16. The later accumulation of AVP in the parvocellular neurons may be related with their late withdrawal from the mitotic cycle as compared to the magnocellular neurons [28, 29, 31, 33]. This delay might imply a less significant physiological importance of the SCN than the SON, RCN and PVN during perinatal period. Because parvocellular neurons are known to project their axons to the forebrain and brain stem [7, 8], but not to the PN and ME, they may not be related to the regulation of water and electrolyte metabolism. It is likely that AVP in the SCN neurons begin to function as a neurotransmitter after birth, concomitant with their increase in AVP immunoreactivity.

The adult-type distribution pattern of SON neurons completes during fetal life, that is, more AVP neurons are present in the caudal region of the SON than the rostral region. This particular distribution pattern has also been shown in the rat [34].

The occurrence of bead-like deposits along the axons implies the active transport of neurosecretory material from the hypothalamus to the PN and ME. After birth, many large-sized deposits of Herring bodies could be observed in the axons of the hypothalamo-neurohypophysial tracts. Axonal outgrowth from the PVN neurons also occurred relatively quickly after the appearance of immunoreactivity in the perikarya. AVP-immunoreactive cell bodies were encountered in the SON and PVN on FA 15, and their termini in the external layer of the ME, which recieves projections of AVP-immunoreactive fibers almost exclusively from the PVN [11, 12], were detected on FA 18.

Immunoreactive axons were first observed in the peripheral area of the PN on FA 15. The age of the fetus at which AVP-immunoreactive axons were first detected in the present study was older as compared with the result using neurophysin immunocytochemistry by Silverman *et al.* [32]. The findings in the present study were in harmony with those by Eurenius and Jarskär [17] in that small fiber bundles were found in the PN, primarily in the region bordering the intermediate lobe on FA 14. Their data suggest that axonal outgrowth is initiated at least in some cells very shortly after their arrival at the presumptive locus of the hypothalamic nuclei (the arrival is between FA 13 and FA 14). Our results seem to show that the transport of the AVP begins after the projection of axonal termini reaches the PN. At present we don't know how long the time lag for the transport of AVP from the perikarya to the termini last, but if it is very short, then it is possible that the hormone is present in the growth cone, the very front of the axonal growth. Previous studies suggested that the fetal PN is a heterogeneous structural entity and that there are distinct territories for ingrowing fibers [17, 32]. Present observations also demonstrated that in the fetal PN AVP-immunoreactive axons were exclusively present in the peripheral area. The fact that the central area of the developing PN was occupied by proliferating pituicytes may have some is closely related to the peripheral distribution of growing fibers.

The present study clarified the developmental events of AVP-immunoreactive neurons of the mouse HNS. To sum up, the present results show that (1) there may be a time lag between the withdrawal from mitotic cycle and the initiation of peptide synthesis in AVP neurons, that (2) the HNS develops rapidly to attain the adult-like pattern during fetal life, and that (3) the HNS nearly attains complete maturity by the time of weaning.

REFERENCES

1 Vandesande, F. and Dierickx, K. (1975) Identification of the vasopressin producing and of the oxyto-

cin producing neurons in the hypothalamic magnocellular neurosectetory system of the rat. Cell Tissue Res., **164**: 153–162.

2 Choy, V. J. and Watkins, W. B. (1977) Immunocytochemical study of the hypothalamo-neurohypophysial system. II. Distribution of neurophysin, vasopressin and oxytocin in the normal and osmotically stimulated rat. Cell Tissue Res., **180**: 467–490.

3 Sofroniew, M. V., Weindl, A., Schinko, I. and Wetzstein, R. (1979) The distribution of vasopressin-, oxytocin-, and neurophysin-producing neurons in the guinea pig brain. Cell Tissue Res., **196**: 367–384.

4 Rhodes, C. H., Morrell, J. I. and Pfaff, D. W. (1981) Immunohistochemical analysis of magnocellular elements in rat hypothalamus: Distribution and numbers of cells containing neurophysin, oxytocin, and vasopressin. J. Comp. Neurol., **198**: 45–64.

5 Kawamoto, K. (1985) Immunohistochemical localization of vasopressin and oxytocin neurons in the mouse hypothalamus. J. Sci. Hiroshima Univ., Ser. B, Div. 1, **32**: 25–33.

6 Brownstein, M. J., Russell, J. T. and Gainer, H. (1980) Synthesis, transport, and release of posterior pituitary hormones. Science, **207**: 373–378.

7 Hoorneman, E. M. D. and Buijs, R. M. (1982) Vasopressin fiber pathways in the rat brain following suprachiasmatic nucleus lesioning. Brain Res., **243**: 235–241.

8 Zimmerman, E. A., Nilaver, G., Hou-Yu, A. and Silverman, A. J. (1984) Vasopressinergic and oxytocinergic pathways in the central nervous system. Fed. Proc., **43**: 91–96.

9 Vandesande, F., De Mey, J. and Dierickx, K. (1974) Identification of neurophysin producing cells. I. The origin of the neurophysin-like substance-containing nerve fibres of the external region of the median eminence of the rat. Cell Tissue Res., **151**: 187–200.

10 Dierickx, K., Vandesande, F. and De Mey, J. (1976) Identification, in the external region of the rat median eminence, of separate neurophysin-vasopressin and neurophysin-oxytocin containing nerve fibres. Cell Tissue Res., **168**: 141–151.

11 Vandesande, F., Dierickx, K. and De Mey, J. (1977) The origin of the vasopressinergic and oxytocinergic fibers of the external region of the median eminence of the rat hypophysis. Cell Tissue Res., **180**: 443–452.

12 Antunes, J. L., Carmel, P. W. and Zimmerman, E. A. (1977) Projections from the paraventricular nucleus to the zona externa of the median eminence of the rhesus monkey: An immunohistochemical study. Brain Res., **137**: 1–10.

13 Lang, R. E., Heil, J., Ganten, D., Hermann, K., Rascher, W. and Unger, Th. (1983) Effects of lesions in the paraventricular nucleus of the hypothalamus on vasopressin and oxytocin contents in brainstem and spinal cord of rat. Brain Res., **260**: 326–329.

14 Hawthorn, J., Ang, V. T. and Jenkins, J. S. (1985) Effects of lesions in the hypothalamic paraventricular, supraoptic and suprachiasmatic nuclei on vasopressin and oxytocin in rat brain and spinal cord. Brain Res., **346**: 51–57.

15 Rinne, U. K. and Kivalo, E. (1965) Maturation of hypothalamic neurosecretion in rat, with special reference to the neurosecretory material passing into the hypophysial portal system. Acta Neuroveget., **27**: 166–183.

16 Paull, W. K. (1973) A light and electron microscopic study of the development of the neurohypophysis of the fetal rat. Anat. Rec., **175**: 407–408.

17 Eurenius, L. and Jarskär, R. (1974) Electron microscopy of neurosecretory nerve fibres in the neural lobe of the embryonic mouse. Cell Tissue Res., **149**: 333–347.

18 Galabov, P. and Schiebler, T. H. (1978) The ultrastructure of the developing neural lobe. Cell Tissue Res., **189**: 313–329.

19 Gash, D., Sladek, C. and Scott, D. (1980) Cytodifferentiation of the supraoptic nucleus correlated with vasopressin synthesis in the rat. Brain Res., **181**: 345–355.

20 Kawamoto, K., Yamada, Y. and Kawashima, S. (1984) Immunohistochemical and electron microscopic studies on the development of the mouse posterior lobe. Zool. Sci., **1**: 980 (Abstract).

21 Silverman, A. J. (1975) The hypothalamic magnocellular neurosecretory system of the guinea pig. II. Immunohistochemical localization of neurophysin and vasopressin in the fetus. Am. J. Anat., **144**: 445–460.

22 Wolf, G. and Trautmann, B. (1977) Ontogeny of the hypothalamo-neurohypophysial system in rats — an immunohistochemical study. Endokrinologie, **69**: 222–226.

23 Choy, V. J. and Watkins, W. B. (1979) Maturation of the hypothalamo-neurohypophysial system. I. Localization of neurophysin, oxytocin and vasopressin in the hypothalamus and neural lobe of the developing rat brain. Cell Tissue Res., **197**: 325–336.

24 Sinding, C., Robinson, A. G., Seif, S. M. and Schmid, P. G. (1980) Neurohypophyseal peptides in the developing rat fetus. Brain Res., **195**: 177–186.

25 Sinding, C., Seif, S. M. and Robinson, A. G. (1980) Levels of neurohypophyseal peptides in the rat during the first month of life. I. Basal levels in plasma, pituitary, and hypothalamus. Endocrinology, **107**: 749–754.

26 Hsu, S.-M., Raine, L. and Fanger, H. (1981) Use of avidin-biotin-peroxidase complex (ABC) in immunoperoxidase techniques: A comparison between ABC and unlabeled antibody (PAP) procedures. J. Histochem. Cytochem., **29**: 577–580.

27 Kawamoto, K. and Kawashima, S. (1986) Effects of glucocorticoids and vasopressin on the regeneration of neurohypophyseal hormone-containing axons after hypophysectomy. Zool. Sci., **3**: 723–736.

28 Ifft, J. D. (1972) An autoradiographic study of the time of final division of neurons in the rat hypothalamic nuclei. J. Comp. Neurol., **144**: 193–204.

29 Okamura, H., Fukui, K., Koyama, E., Tsutou, H. L. O., Tsutou, T., Terubayashi, H., Fujisawa, H. and Ibata, Y. (1983) Time of vasopressin neuron origin in the mouse hypothalamus: Examination by combined technique of immunocytochemistry and [^{3}H]thymidine autoradiography. Dev. Brain Res., **9**: 223–226.

30 Shimada, M. and Nakamura, T. (1973) Time of neuron origin in mouse hypothalamic nuclei. Exp. Neurol., **41**: 163–173.

31 Altman, J. and Bayer, S. A. (1978) Development of the diencephalon in the rat. II. Correlation of the embryonic development of the hypothalamus with the time of origin of its neurons. J. Comp. Neurol., **182**: 973–994.

32 Silverman, A. J., Goldstein, R. and Gadde, C. A. (1980) The ontogenesis of neurophysin-containing neurons in the mouse hypothalamus. Peptides, **1**: 27–44.

33 Anderson, C. H. (1978) Time of neuron origin in the anterior hypothalamus of the rat. Brain Res., **154**: 119–122.

34 Swaab, D. F., Nijveldt, F. and Pool, C. W. (1975) Distribution of oxytocin and vasopressin in the rat supraoptic and paraventricular nucleus. J. Endocrinol., **67**: 461–462.

ZOOLOGICAL SCIENCE 5: 1033–1042 (1988)

Molecular- and Immuno-histochemical Study on Expressions of Vasopressin and Oxytocin Genes Following Sodium Loading

Susumu Hyodo[1], Mamoru Fujiwara, Moriyuki Sato[2] and Akihisa Urano[1]

Department of Regulation Biology, Faculty of Science, Saitama University, Urawa, Saitama 338, and [2]Tokyo Research Labolatories, Kyowa Hakko Kogyo Co., Machida, Tokyo 194, Japan

ABSTRACT—We investigated the effects of drinking hypertonic saline on expressions of vasopressin (AVP) and oxytocin (OXT) genes in neurosecretory neurons of the supraoptic (SON) and the paraventricular (PVN) nuclei in rats with the oligonucleotide-mRNA *in situ* hybridization and the immunohistochemical avidin-biotin-peroxidase complex (ABC) methods. Autoradiographic hybridization signals that indicate the localization of AVP mRNA were significantly increased in the SON 4 days after the commencement of the sodium loading, while the signal increase in the PVN was less conspicuous than that in the SON. Signals for OXT mRNA in both the SON and the PVN were rapidly increased and attained to a peak level by the second day after the onset of sodium loading. In the hypothalamic sections adjacent to those used for *in situ* hybridization, the number of immunoreactive (ir) AVP neurons was decreased in the PVN by day 7. The percentage of heavily stained AVP neurons to all ir-AVP ones was decreased in the SON by day 7. Changes in the number of ir-OXT neurons and the percentage of heavily stained OXT neurons were insignificant. Significant hypertrophy was found in both AVP and OXT neurons in the SON and the PVN after day 2. The present results thus indicate that the AVP and OXT mRNAs are increased by sodium loading. It is probable that supraoptic AVP neurons are more sensitive to changes in extracellular sodium concentration than paraventricular AVP neurons, and that OXT neurons have some physiological role in the water and salt metabolism.

INTRODUCTION

Arginine vasopressin (AVP) and oxytocin (OXT), mammalian neurohypophysial hormones, are synthesized in the hypothalamic magnocellular neurosecretory neurons, transported mainly to the neurohypophysis, and are released into the circulation. Following a rise in plasma osmolality or plasma Na^+ concentration, the number of action potentials in magnocellular AVP neurons and the plasma level of AVP were increased [1]. OXT release was also stimulated by sodium loading [2–4]. OXT could stimulate electrolyte excretion [2]. It is possible that OXT is involved in the regulation of water and salt metabolism, although any physiological significances of OXT for water and salt metabolism have not been clarified yet.

Chronic water deprivation and sodium loading elevated amino acid incorporation into the neurosecretory neurons [5, 6]. These stimuli further induced cytological changes in these neurons, e.g., hypertrophy, an increase in nuclear and nucleolar diameters, dilation of endoplasmic reticulum, and an increase in the number of free ribosomes [7]. These data strongly suggest that biosyntheses of the neurohypophysial hormones are elevated by water deprivation and sodium loading. Nevertheless, the intensity of immunoreactivity, especially that in AVP neurons, was decreased by these stimuli [8]. An investigation of gene expressions is thus required for further understanding of the biosynthetic activity of AVP and OXT neurons.

Accepted January 22, 1988
Received December 18, 1987

[1] Present address: Ocean Research Institute, University of Tokyo, Minamidai, Nakano-ku, Tokyo 164, Japan.

Since an *in situ* hybridization (ISH) method can be an appropriate method for a gene expression study, we have developed an ISH method using synthetic oligonucleotide probes which can discriminate the AVP mRNA from the highly homologous OXT mRNA [9–11]. Several investigators including us have now clarified using various hybridization methods that the AVP mRNA is increased by sodium loading and water deprivation [10–18]. The OXT mRNA is also increased by sodium loading and water deprivation [17, 19]. However, at present, little information has been available concerning the time courses of changes in AVP and OXT gene expressions, especially those of alterations in cellular and immunocytochemical aspects of neurosecretory neurons. Such information is the indispensable requisite for understanding how AVP and OXT neurons in the supraoptic (SON) and paraventricular (PVN) nuclei are involved in osmoregulation.

In the present study, changes in the levels of AVP and OXT mRNAs in magnocellular neurons of the rat hypothalamus were examined after oral intake of hypertonic saline for 2 to 7 days with the ISH method using synthetic oligonucleotide probes. Furthermore, adjacent tissue sections were immunohistochemically stained, and stainability and sizes of single AVP and OXT immunoreactive neurons were determined. Preliminary results appeared elsewhere [13, 17].

MATERIALS AND METHODS

Animals

Male Wistar-Imamichi rats (Imamichi Institute for Animal Reproduction, 140–160 g) were housed in individual cages with 14L: 10D light schedule. Animals were allowed free access to tap water and standard laboratory chow (Charles River) for at least 3 days prior to the start of the experiment. They were then divided into 4 experimental groups, each of them included 7 rats, and were given orally a 2% sodium chloride solution as drinking water for 0, 2, 4 and 7 days prior to sacrifice. A preliminary study showed that effects of sodium loading on AVP gene expression first appeared on the second day of treatment [13]. Daily water intakes and urine volumes were measured and urine samples were kept at −20°C to determine their osmolality and Na^+ concentration. The animals were killed by decapitation between 10: 00 to 12: 00 to avoid possible circadian fluctuations in AVP and OXT gene expressions [20]. Their hypothalami and pituitaries were immediately removed and were immersed in a fixative solution containing 2% paraformaldehyde, 1% glutaraldehyde and 1% picric acid in 0.05 M phosphate buffer (pH 7.3). At the same time, blood was collected and centrifuged. Plasma samples were stored at −20°C. Plasma and urine Na^+ concentrations were measured later with an atomic absorption spectrometer (Hitachi 180-50). Their osmolality was determined by the freezing point method.

In situ hybridization and quantitation of autoradiographic signals

The individual tissues were paraffin-sectioned, divided into several groups, and were processed for *in situ* hybridization and immunohistochemistry. The precise procedures for tissue preparation and ISH were described previously [9]. Two types of 22mer synthetic deoxyoligonucleotide probes, complementary to the loci of rat mRNAs encoding AVP-neurophysin (NP) (1–8) and OXT-NP (1–8), were used in this study. For semiquantitative expression of hybridization signals, the numbers of autoradiographic silver grains in 100 μm × 100 μm squares settled in each of the SON and the PVN (Fig. 1) were counted. Then the numbers of grains in the areas adjacent to the SON and the PVN, that is, the background levels, were counted, and were subtracted from the corresponding values in the SON and the PVN. Thereafter, the single cellular numbers of grains were calculated by dividing the specific number of silver grains by the numbers of immunoreactive neurons within the 100 μm × 100 μm squares.

Immunohistochemistry

The sections adjacent to those used for grain counting were immunohistochemically stained by the avidin-biotin-peroxidase complex (ABC) method, the detailed procedure of which was described previously [21]. Specificity tests of im-

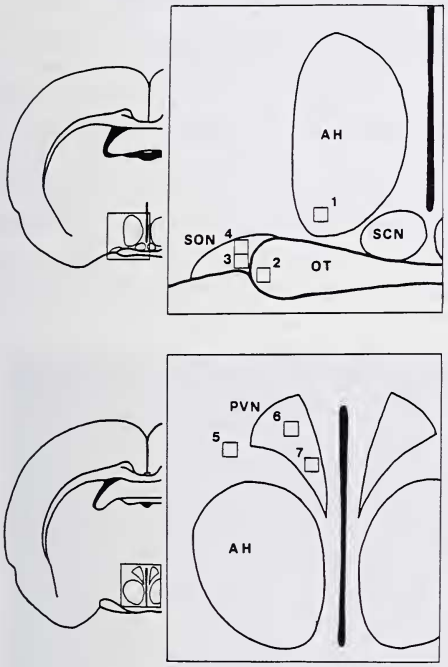

FIG. 1. Schematic diagram showing the loci of 100 μm × 100 μm squares in which autoradiographic signals were quantitated. The numbers of silver grains in regions 3 (AVP region in the SON), 4 (OXT region in the SON), 6 (AVP region in the PVN), and 7 (OXT region in the PVN) were counted, and then the numbers of grains in the adjacent squares (2 and 5) were subtracted to obtain the specific numbers of signals. The numbers of grains in the regions 2 and 5, which are fibrous neuropil areas, were statistically in the same range with that in the anterior hypothalamic nucleus (AH, 1). OT, optic tract; SCN, suprachiasmatic nucleus.

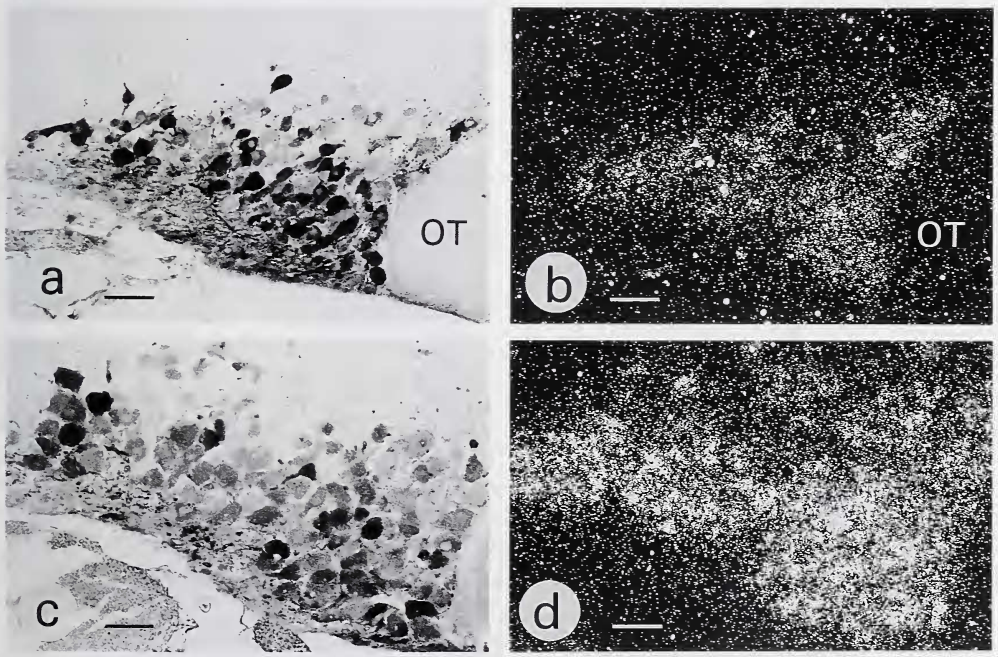

FIG. 2. AVP immunoreactive (ir) neurons and *in situ* hybridization of AVP mRNA in the SON of normal (a, b) and 7-day sodium loaded rats (c, d). Note the density of silver grains over the SON of the sodium loaded rat (d) is higher than that in the control rat (b). On the contrary, stainability of ir-AVP neurons in the sodium loaded rat (c) is reduced from that in the control rat (a). OT, optic tract. Scale bar, 50 μm.

munohistochemistry were also described previously [9, 11]. The ABC method is considered to be superior than the peroxidase-antiperoxidase (PAP) method for a quantitative study [21]. In this study, primary antisera were used as follows: rabbit anti-AVP (UCB-Bioproducts) was diluted 1: 32,000 with phosphate buffered saline containing 0.5% BSA (PBS-BSA, pH 7.6) and rabbit anti-OXT (a gift from Professor S. Kawashima, Hiroshima University) was diluted 1: 20,000 with PBS-BSA. These values for dilution gave half-maximal staining of AVP and OXT neurons in normal non-treated rats, and are considered to be theoretically appropriate for quantitative immunohistochemistry by an analogy of radioimmunoassay. The values for dilution were determined by serial dilution experiments. Submaximally stained and faintly stained sections were first selected by microscopic observation. By comparison with them, the medially stained section was singled out

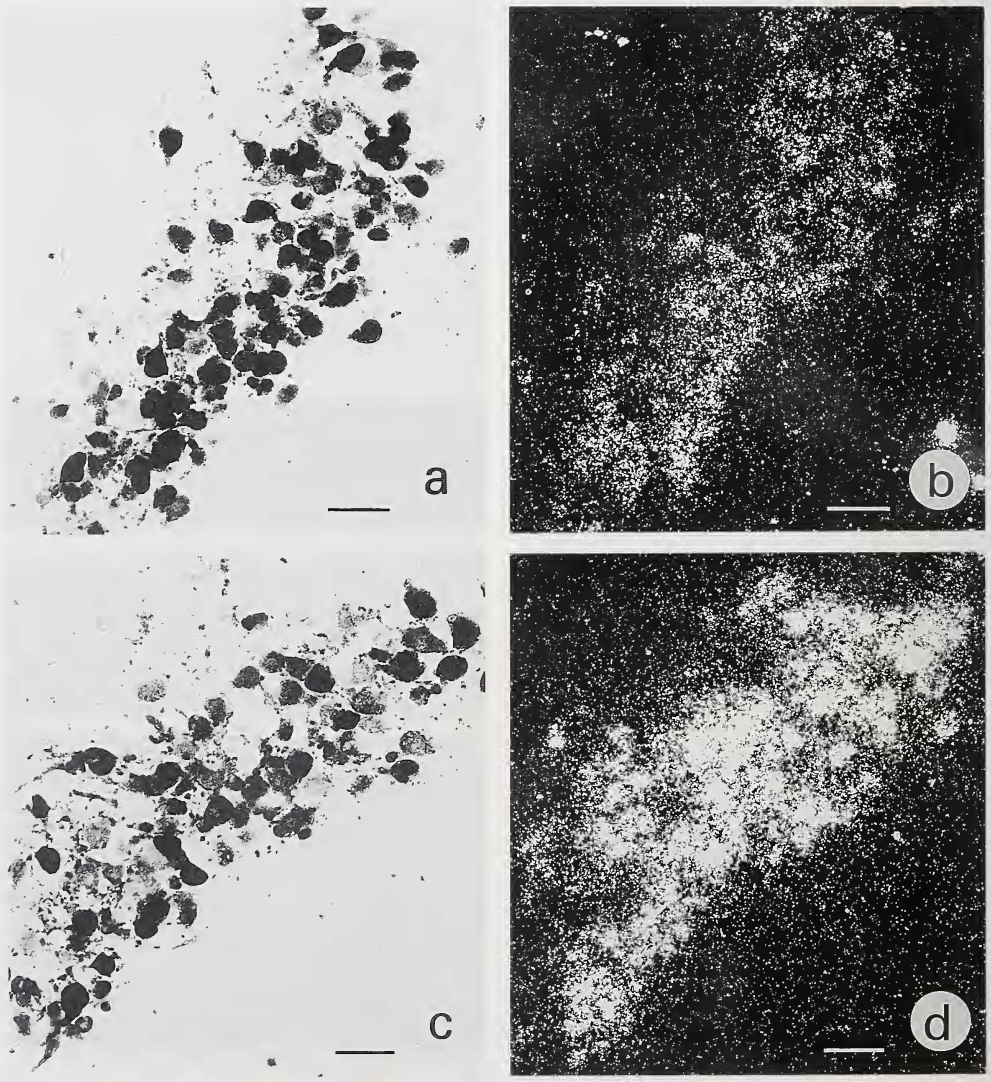

Fig. 3. OXT immunoreactive neurons and *in situ* hyridization of OXT mRNA in the PVN of normal (a, b) and 2-day sodium loaded rats (c, d). Note the density of silver grains over the PVN of the sodium loaded rat (d) is higher than that in the control rat (b). Scale bar, 50 μm.